Available online at www.sciencedirect.com
SCIENCE DIRECT®
Bioorganic & Medicinal Chemistry Letters 14 (2004) 4445–4448
Bioorganic & Medicinal Chemistry Letters

Discovery of inhibitors of human adipocyte fatty acid-binding protein, a potential type 2 diabetes target

Fredik Lehmann,[a] Saba Haile,[b] Eva Axen,[b] Carmen Medina,[c] Jonas Uppenberg,[c] Stefan Svensson,[c] Thomas Lundbäck,[b] Lena Rondahl[d] and Tjeerd Barf[a,*]

[a]*Department of Medicinal Chemistry, Biovitrum AB, SE-751 37 Uppsala, Sweden*
[b]*Department of Assay Development and Screening, Biovitrum AB, SE-751 37 Uppsala, Sweden*
[c]*Department of Structural Chemistry, Biovitrum AB, SE-751 37 Uppsala, Sweden*
[d]*Department of Biology, Biovitrum AB, SE-751 37 Uppsala, Sweden*

Received 16 February 2004; revised 14 June 2004; accepted 17 June 2004

Abstract—Low micromolar human A-FABP inhibitors were found by utilizing a fluorescence polarization assay, X-ray crystallography and modeling. The carbazole- and indole-based inhibitors displayed approximately 10-fold preferences over human H-FABP and E-FABP, and are highly selective against I-FABP. This communication describes the SAR for drug-like synthetic inhibitors of human A-FABP.

Fatty acid-binding proteins (FABPs) are ~15 kDa cytoplasmic proteins expressed in a highly tissue-specific manner and bind to endogenous fatty acids. Although the role of FABPs is still fairly unclear, it has been suggested that they act as fatty acids shuttles.[1] Fatty acids are transported by FABPs from the cell surface to the various sites of metabolism or storage. The total content of FABP in fat cells is directly correlated with the rate of lipolysis, and this seems to be partly mediated by the FABP-hormone-sensitive lipase interaction.[2] Recently it has been shown that mice with a null mutation in adipocyte FABP (A-FABP) developed obesity on a high-fat diet without the concomitant insulin resistance as seen in the wild-type mice.[3] The high-fat fed A-FABP deficient mice demonstrated significantly lower plasma glucose and insulin levels and better performance in both insulin and glucose tolerance tests.[4] Thus displacement of the endogenous A-FABP-bound fatty acids by a small molecule could potentially produce a similar 'phenotype' as the A-FABP null mice. Although inhibition of A-FABP offers in theory an interesting and novel approach for the treatment of Type 2 diabetes, the inhibitor may have to be selective over certain other members of the FABP family. Notably, mice with a disruption in the gene encoding for the heart or muscle variant H-FABP were reported to suffer from stress-intolerability, in a few cases leading to death.[5] Ironically, the overall sequence identity of human A-FABP and H-FABP is 65%, being the highest degree of homology among the known human FABPs.[6] Comparison of the binding sites of these two FABPs reveals only a handful of amino acid differences.

Previously, A-FABP inhibitors were claimed in a number of patent applications submitted by Bristol–Myers Squibb, but no binding data were disclosed.[7] We set out to find compounds that can effectively and selectively displace naturally occurring human A-FABP ligands, using a fluorescence polarization assay.[8] Although the search for selective A-FABP inhibitors is potentially difficult due to the reasons mentioned above,

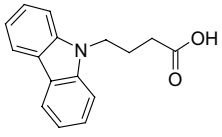

1

Figure 1. Hit compound **1**.

Keywords: A-FABP inhibitors; FABP4.
* Corresponding author. Tel.: +46-8-69-73885; fax: +46-8-69-73914; e-mail: tjeerd.barf@biovitrum.com

0960-894X/$ - see front matter © 2004 Elsevier Ltd. All rights reserved.
doi:10.1016/j.bmcl.2004.06.057

Table 1. Selectivity profile of fatty acid analogs[a]

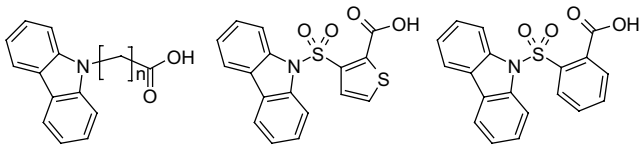

1-4 **5** **6**

Compound	*n*	A-FABP IC_{50} (μM)	H-FABP IC_{50} (μM)	E-FABP IC_{50} (μM)	I-FABP IC_{50} (μM)
PA	—	0.93	2.6	1.2	1.7
3	1	>100	—	—	—
2	2	9.4	5.7	30	—
1	3	0.57	<0.6[14]	6.7	>100
4	4	0.8	—	3.0	—
5[15]	—	1.1	9.9	9.1	42
6	—	4.3	42	17	>100

[a] In vitro binding data are reported as the mean of triplicate experiments performed on the same dilution.

we demonstrate in this communication that selectivity is not necessarily an issue.

Carbazole butanoic acid (**1**) was identified as a hit for human A-FABP from a high-throughput-screen, with an IC_{50} of approximately 0.6 μM (Fig. 1, Table 1). This is in the binding range of some of the anticipated endogenous ligands such as palmitic acid (PA). Some immediate modifications focused on alkyl chain-shortened and elongated analogues. Shortening the linker chain by one carbon yielded a loss in potency (**2**, IC_{50} 9.4 μM), whereas one methylene linker unit as in **3** totally abolished human A-FABP inhibition. Elongation to the four-carbon linker resulted in retained potency (IC_{50} 0.8 μM). These synthetic inhibitors possessed no selectivity against H-FABP. Yet, **1** showed a ~12-fold preference against human epithelial FABP (E-FABP), and compounds of this type were shown to be poor binders of human intestinal FABP (I-FABP).

With these facts in hand, a co-crystal structure of **1** with human A-FABP was resolved, which enabled us to design compounds with even less fatty acid like properties. Crystals of human A-FABP were grown with the hanging drop method. A drop contained 2 mL of protein at 20 mg/mL in 25 mM Tris pH 8.0, 5% DMSO, 1 mM ligand, and 2 mL from the reservoir, containing 20% PEG 2000, 5% DMSO, and 0.1 M Tris pH 7.0. A complete data set to 2.0 Å resolution was collected on a single crystal. The crystal belonged to the space group $P2_12_12$ with cell dimensions $a = 72.1$, $b = 53.0$, and $c = 31.8$ Å. Crystals were cryofrozen in mother liquor and data were collected on a Raxis4 image plate mounted on a Rigaku generator with a rotating copper anode. It was processed with the programs Denzo and Scalepack.[9] The A-FABP structure was solved by molecular replacement using mouse A-FABP as a model (PDB code: 1lie). Model building was performed with O.[10] The model was refined with Refmac.[11] The final model has an *R*-factor of 0.200 and a free *R*-factor of 0.276. R_{merge} and completeness were calculated by Scalepack (Crystallographic coordinates have been deposited with the Protein Data Bank, PDB code: 1tow).

The complex reveals that **1** binds in a very similar fashion to long chain fatty acids (Fig. 2). The carboxylic acid interacts strongly with Arg126 and Tyr128, whereas the folded carbon linker and the carbazole moiety follow a lipophilic motif in the binding pocket, as the natural ligands do.[12] A major difference is that with oleic acid

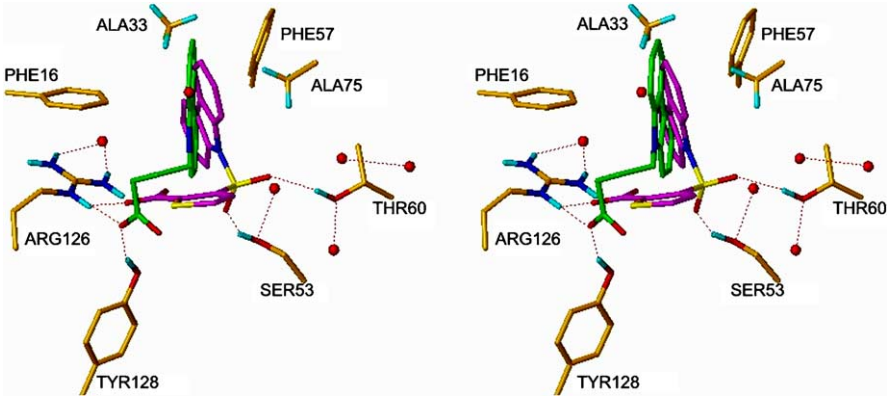

Figure 2. Stereo view of the binding pocket of **1** (green) co-crystallized in human A-FABP and the docked overlay with **5** (magenta).

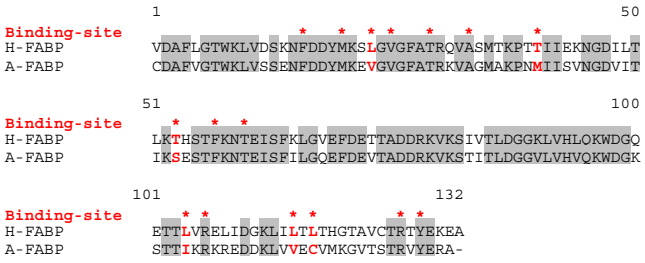

Figure 3. Sequence alignment of human A-FABP and H-FABP. The sequence identity is 65% (grey-highlighted). Marked with an asterix are the binding-site residues and in red bold, those that differ in both proteins.

bound to the holoform, residue Phe57 in the portal region is pushed away by the hydrocarbon tail. Since **1** is contained within the binding site, Phe57 blocks the entrance of the cavity as observed in the apoprotein. Since the major amino acid differences between human A-FABP and H-FABP can be found near the linker portion of **1**, it is reasonable to assume that further modification of this moiety will influence the preference for either FABP. For instance, the methylene units are in close proximity to Val115 and Cys117 of A-FABP, whereas both these amino acids are substituted by leucines in H-FABP (Fig. 3). Other differences of interest in this part of the binding pocket are M40T, S53T, and I104L.

The crystal structure of the A-FABP–(**1**) complex was used as a starting point for docking studies of a limited set of virtual compounds. This set comprised compounds in which the flexible butanoic acid residue of **1** was exchanged with positional isomers of benzoic acids, benzyl carboxylic acids, sulfonylthiophene carboxylic acids, and sulfonyl benzoic acids. The binding site of FABP contains many water molecules even in the presence of a ligand and it is therefore important to investigate the effect of different water configurations in the docking results. To this end, four binding sites were constructed where sets of 1, 6, 8, and 14 crystal waters were included during the docking procedure.[13] The comparison of the four dockings shows that too many water molecules prevent the virtual binder from finding docking modes that allow for the important interactions to take place. On the other hand, the inclusion of some water molecules may direct the ligand into a better binding mode by space filling and allowing for favorable H-bond bridging. Of the four computer experiments, the one with six water molecules in the binding site gave the best binding poses. (It is worth mentioning that in this experiment two different binding modes of **1** were found: The one in the crystal structure, and another where the carbazole group lies perpendicular to **1** along the direction of the alkyl chain). The most reliable binding modes were considered the ones that positioned the carboxylic acid in the vicinity of the Arg126 and Tyr128 residues.

From the virtual set, aryl sulfonamides **5** and **6** were extracted as interesting candidates following the modeling exercise. For example, the sulfonyl group of **5** is predicted to pick up potential hydrogen bonds with Ser53

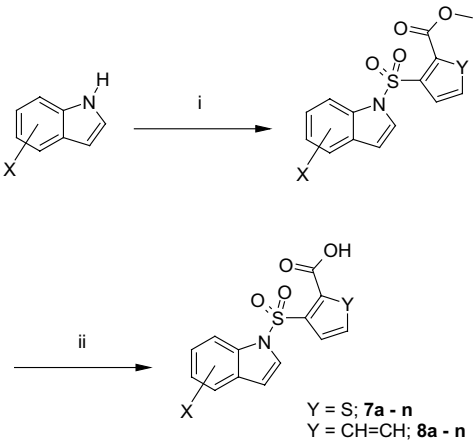

Scheme 1. Reagents and conditions: (i) NaH, DMF, methyl 3-chlorosulfonylthiophene-2-carboxylate or methyl 2-(chlorosulfonyl) benzoate; (ii) THF, MeOH, LiOH (2 M).

and Thr60 (Fig. 2). Indeed, **5** displayed an IC_{50} value of 1.1 μM in the range of **1** (Table 1), whereas **6** proved to be about 4-fold less active. Both **5** and **6**, have an improved selectivity profile as compared to the mother compound with approximately a 10-fold preference for A-FABP over H-FABP (Table 1). Interestingly, both human H-FABP and E-FABP have a S53T substitution in this position as compared to A-FABP, making the interaction of the threonine OH less susceptible.

Subsequently, a number of N-indole derivatives were prepared to investigate the influence of different aryl substituents. The sulfonylthienyl and sulfonylbenzene moieties were used as the 'linker mimetics'. All tested substances were prepared by treating carbazole or commercially available indoles with NaH in DMF, followed by addition of the aryl sulfonyl chloride (Scheme 1). Subsequent hydrolysis of the ester was achieved using a mixture of equivalent amounts of THF, MeOH, and aqueous lithium hydroxide (2 M). These mild conditions were chosen to avoid hydrolysis of the sulfonamide bond in the thiophene series. The final compounds were purified using preparative HPLC, and characterized by ^{1}H NMR, HPLC and mass spectroscopy. Compounds **7a**–**8n** were evaluated for their affinity toward A-FABP, and the results are shown in Table 2.

The sulfonylthiophene derivatives displayed generally a 2- to 9-fold better inhibitory activity than the compounds that possess the sulfonylbenzene group as a spacer (Table 2). A methyl at the 3- or 6-position of the indole (**7a** and **7d**) resulted in the best A-FABP inhibitors with IC_{50} values close to 1 μM. The 3-methyl of **7a** could potentially occupy the same space as one of the benzene rings of the carbazole. There seems to be room for small substituents like the methyl or methoxy in the 6- or 7-position of the indole (**7d**,**g**, and **7h**), whereas substitution at the 4- and 5-position is less well tolerated. An exception is the 5-bromo derivative **7m** with an IC_{50} value in the order of 1 μM. Compound **7m** was profiled against the other FABPs and was found to retain the preference for H-FABP (IC_{50} 9.8 μM) and

Table 2. A-FABP inhibitory potency of indole derivatives[a]

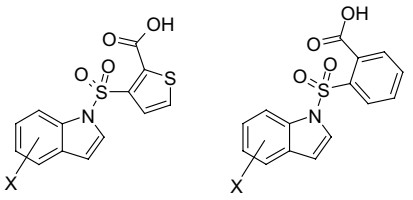

7a - n **8a - n**

X	Compound	A-FABP IC_{50} (μM)	Compound	A-FABP IC_{50} (μM)
3-Me	**7a**	1.5	**8a**	8.5
4-Me	**7b**	7.4	**8b**	12
5-Me	**7c**	7.1	**8c**	30
6-Me	**7d**	1.3	—	—
4-O-Me	**7e**	13	**8e**	89
5-O-Me	**7f**	10	—	—
6-O-Me	**7g**	2.6	**8g**	6.1
7-O-Me	**7h**	2.6	—	—
4-F	—	—	**8i**	10
5-F	**7j**	3.5	—	—
6-F	**7k**	4.7	—	—
7-F	**7l**	4.5	—	—
5-Br	**7m**	1.3	**8m**	12
3-acetamide	**7n**	32	**8n**	>100

[a] In vitro binding data are reported as the mean of triplicate experiments performed on the same dilution.

E-FABP (IC_{50} 14 μM), respectively. To our surprise, **7m** also inhibited I-FABP quite potently with an IC_{50} value of 3.9 μM.

In summary, the carbazole- and indole-based derivatives presented are the first synthetic and drug-like fatty acid analogues that exhibit low micromolar A-FABP inhibitory properties. Modest SAR efforts that involved X-ray crystallography and modeling, resulted in approximately 10-fold preferences against human H-FABP and E-FABP. The carbazole analogues were in addition clearly selective over human I-FABP. Future activities on these potential leads will focus on optimization of potency and selectivity.

References and notes

1. For a review see: (a) Storch, J.; Thumser, A. E. A. *Biochim. Biophys. Acta* **2000**, *1486*, 28–44; (b) Hertzel, A. V.; Bernlohr, D. A. *TEM* **2000**, *11*, 175–180.
2. Jenkins-Kruchten, A. E.; Bennaars-Eiden, A.; Ross, J. R.; Shen, W.-J.; Kraemer, F. B.; Bernlohr, D. A. *J. Biol. Chem.* **2003**, *278*, 47636–47643.
3. Hotamisligil, G. S.; Johnson, R. S.; Distel, R. J.; Ellis, R.; Papaioannou, V. E.; Spiegelman, B. M. *Science* **1996**, *274*, 1377–1379.
4. Uysal, K. T.; Scheja, L.; Wiesbrock, S. M.; Bonner-Weir, S.; Hotamisligil, G. S. *Endocrinology* **2000**, *141*, 3388–3396.
5. Binas, B.; Danneberg, H.; McWhir, J.; Mullins, L.; Clark, A. J. *FASEB J.* **1999**, *13*, 805–812.
6. Veerkamp, J. H.; Peters, R. A.; Maatman, R. *Biochim. Biophys. Acta* **1991**, *1081*, 1–24.
7. (a) Robl, J. A.; Parker, R. A.; Biller, S. A.; Jamil, H.; Jacobson, B. L.; Kodukula, K. WO 200015229 and WO 200015230; (b) Robl, J. A.; Sulsky, R. B.; Magnin, D. R. WO 200059506; (c) Sulsky, R.; Robl, J. A. WO 200154694 and WO 200240448.
8. For experimental details, see: Van Dongen, M. J. P.; Uppenberg, J.; Svensson, S.; Lundbäck, T.; Åkerud, T.; Wikström, M.; Schultz, J. *J. Am. Chem. Soc.* **2002**, *124*, 11874–11880, The fluorescence polarization assay described herein was used with minor modifications.
9. Otwinowski, Z.; Minor, W. In *Methods in Enzymology: Macromolecular Crystallography, Pt A*; Academic: San Diego, 1997; Vol. 276, pp 307–326.
10. Jones, T. A.; Zou, J. Y.; Cowan, S. W.; Kjeldgaard, M. *Acta Crystallogr. A* **1991**, *47*, 110–119.
11. Bailey, S. *Acta Crystallogr. Sect. D. Biol. Crystallogr.* **1994**, *50*, 760–763.
12. Xu, Z.; Bernlohr, D. A.; Banaszak, L. J. *J. Biol. Chem.* **1993**, *268*, 7874–7884.
13. All the dockings were done with the ICM program version 3.0, MolSoft L.L.C. For a description of the method, see: Abagyan, R.; Totrov, M.; Kuznetsov, D. *J. Comp. Chem.* **1994**, *15*, 488–506.
14. The sensitivity of the fluorescence polarization assay is limited by the total protein concentration, which ranges from sub-μM to low μM depending on the FABP isoform. In this case the measured potency approaches the total protein concentration and hence the value may represent an underestimation of the potency.
15. *3-(9H-Carbazol-9-ylsulfonyl)thiophene-2-carboxylic acid* (**5**): Under N_2-atm, carbazole (300 mg, 1.80 mmol) was dissolved in DMF (5 mL) and NaH (52 mg, 2.16 mmol) was added. After 5 min, methyl 3-chlorosulfonylthiophene-2-carboxylate (520 mg, 2.16 mmol) was added and the reaction mixture was stirred at ambient temperature for 1 h. The reaction mixture was poured into water (20 mL) and the precipitate that formed was filtered off, air-dried, and recrystallized from ethanol (white needles, 360 mg, 59%). The intermediate methyl ester (200 mg, 0.54 mmol) was then added to a mixture of THF (1 mL) and aq LiOH (2 M, 1 mL) and stirred for 4 h. The reaction mixture was acidified until pH 3–4 with aq HCl (1 M) and extracted twice with DCM. The combined organic phases were dried ($MgSO_4$) and evaporated in vacuo affording a white solid. Recrystallization from acetonitrile gave the pure title compound as white prisms (150 mg, 78%). Mp 195–196 °C; HPLC purity 100%; ^{1}H NMR (400 MHz, DMSO-d_6) δ 6.81 (d, 1H, J = 5.3 Hz), 7.41–7.51 (m, 4H), 7.82 (d, 1H, J = 5.5 Hz), 7.98 (d, 2H, J = 8.3 Hz), 8.21 (d, 2H, J = 7.0 Hz); MS-ES (pos) *m/z* 358.